Can slow roll inflation induce relevant helical magnetic fields?

Ruth Durrer, Lukas Hollenstein and Rajeev Kumar Jain

Département de Physique Théorique, Université de Genève, 24, Quai Ernest Ansermet, CH–1211 Genève 4, Switzerland

E-mail: Ruth.Durrer@unige.ch, Lukas.Hollenstein@unige.ch, Rajeev.Jain@unige.ch

Abstract. We study the generation of helical magnetic fields during inflation induced by an axial coupling of the electromagnetic field to the inflaton. During slow roll inflation, we find that such a coupling always leads to a blue spectrum with $B^2 \propto k$. We also show that a short deviation from slow roll does not result in strong modifications to the shape of the spectrum. The magnetic energy density at the end of inflation is too small to back-react on the background dynamics of the inflaton. We calculate the evolution of the correlation length and the field amplitude during the inverse cascade and viscous damping of the helical magnetic field in the radiation era after inflation. The final magnetic fields turn out to be far too weak to provide the seeds for the observed fields in galaxies and clusters.

1. Introduction

Cosmic magnetic fields have been observed on all scales ranging from stars to near and far away galaxies and galaxy clusters [1, 2, 3, 4] and there are even indications that magnetic fields are also present in filaments [5]. The strength of the magnetic fields observed in galaxies and clusters is typically of the order of μGauss. Recently, using the absence of extended emission around TeV blazar gamma-rays, a lower limit of 3×10^{-16} Gauss on the strength of intergalactic magnetic fields was derived [6].

These observations prompt the question of the origin of cosmic magnetic fields. Have they been generated during structure formation or have primordial magnetic fields been amplified? So far, this question has no clear, satisfactory answer. Several studies [7, 8, 9] of second order perturbation theory have shown that up to recombination only very weak magnetic fields of the order of 10^{-20} Gauss and less can be generated by structure formation. Even if these works are to some extent incomplete and even contradictory, it turns out that the magnetic fields from second order perturbation theory are not strong enough to exceed the lower limit derived in Ref. [6]. Whether such fields could have been generated later by the process of galaxy formation and then ejected into intergalactic space remains unclear.

In this work, we pursue the idea that instead magnetic fields are of primordial origin and might have been generated in the early universe. It has been argued that the electroweak or the QCD phase transitions, if they are first order, lead to the generation of magnetic fields [10, 11, 12, 13]. However, causality strongly constrains such fields. Their power spectrum is very blue with $\langle B^2 \rangle \propto k^2$, and therefore, their amplitude on large scales is far too small [14, 15].

On the other hand, if the magnetic fields are produced during inflation, their power spectrum is a priori not constrained by causality but only by the specific model. Since the standard electromagnetic (EM) action is conformally invariant the fluctuations in the EM field are not amplified in the conformally flat expanding background of inflation. Therefore, in order to generate magnetic fields, one needs to break conformal invariance of the EM field, e.g. by coupling the EM field to a scalar or a pseudo-scalar field or to a curvature invariant (for an overview see, for instance, Ref. [16]). Typically, a term of the form fF^2 is considered, where f is a function of time or of the inflaton and F is the EM field tensor. Depending on the form of the coupling f, this coupling gives rise to different magnetic field power spectra, and even scale-invariant spectra are possible (in this context, see Refs. [17, 18]). In this way, the magnetic fields can have sufficient amplitude on large scales to provide seeds for the observed fields in galaxies and clusters. However, the back-reaction on the inflation dynamics, the production of gravitational waves and nucleosynthesis bounds on the amplitude of gravitational waves strongly constrain the magnetic energy density [15, 19].

Quite a different situation is encountered if a coupling to the parity violating term $F\widetilde{F}$, i.e. a term $fF\widetilde{F}$, is added to the standard EM action F^2, where $\widetilde{F}$ is the dual of F. As a consequence, magnetic helicity is generated, which is absent in the case discussed above. This has two interesting aspects: firstly, contrary to non-helical fields, helical fields evolve in the cosmic magnetohydrodynamic (MHD) plasma via inverse cascade [20, 21, 22]. This transfers power from small to large scales so that even blue spectra can lead to significant power on large scales. In Ref. [23], it was shown that the inverse cascade is not quite sufficient for helical fields generated at the electroweak phase transition [24], but it might work for magnetic fields from inflation. Secondly, helical magnetic fields leave a very distinct signature as they violate parity symmetry. This leads to observable effects, e.g. correlations between the anisotropies in the temperature and B-polarisation or in the E- and the B-polarisations in the Cosmic Microwave Background (CMB) [25]. Furthermore, they induce helical gravitational waves [25] which might be observable [26].

Consequences of primordial helical magnetic fields and their generation from primordial helicity have been studied in the past [27, 28]. The interactions of helical magnetic fields and axions have also been investigated [29, 30]. Recently, the generation of helical magnetic fields during inflation in specific models has been studied, e.g. in Ref. [31], helical magnetic fields from N-flation were investigated. In this case, the large number of pseudo-scalar fields driving inflation effectively leads to a large coupling, $f \propto \sqrt{N}$, to the $F\widetilde{F}$ term. In Ref. [32], some toy models for the coupling were analysed

where f was taken to be a power law of kt (k being the wave number and t the conformal time).

In this paper, we study the magnetic fields generated by an axial coupling of the form $f(\phi)F\widetilde{F}$ during inflation, where ϕ is the inflaton. We consider two different forms of the coupling function and show that, contrary to a non-helical coupling of the form $f(\phi)F^2$, a helical coupling always leads to a spectral index $n = 1$ for $B^2 \propto k^n$, as long as slow roll inflation is considered. We also study the effects of a short deviation from slow roll on the magnetic field spectrum and show that such deviations do not strongly modify its shape. We estimate the magnetic energy density as a function of scale and show that back-reaction is typically small. These conclusions are valid for any reasonable coupling function $f(\phi)$. We confirm our analytical results numerically. Even though the inverse cascade in the radiation dominated era after inflation does move power to larger scales, the final power on cosmologically interesting scales is still by far insufficient to provide seeds for the observed magnetic fields in galaxies and clusters. Even if we assume very efficient dynamo amplification.

The remainder of this paper is organised as follows. In the next section, we introduce the axial coupling of the EM field to the inflaton, derive the field equations, discuss the background evolution and the slow roll approximation and derive the linear perturbation equations of the inflaton and the EM vector potential. In Sec. 3, we discuss the evolution equation of the EM quantum fluctuations during inflation and compare the helical to the normal case. In Sec. 4, we solve the equations analytically in the slow roll approximation and calculate the magnetic field spectrum. We also show that as long as the coupling is small, $|f(\phi)| < 1$ so that our perturbative treatment is reliable, one always obtains a spectrum with spectral index $n = 1$. In Sec. 5, we discuss the consequences of a brief violation of the slow roll approximation on the magnetic field spectrum. In Sec. 6, we study the evolution of the magnetic field during the radiation era after inflation. We determine the final spectrum after the inverse cascade. Finally, in Sec. 7, we conclude with a few comments on our results. Two appendices contain some details on the quantisation of the vector potential and the asymptotic behaviour of the Coulomb wave functions, respectively.

Notation & units: We work in a metric with signature $(-+++)$. For tensor components, Greek indices take values $0\ldots3$, while Latin indices run from 1 to 3. The components of spatial 3-vectors with respect to a comoving basis are denoted in bold faces. We employ Heaviside-Lorentz units such that $c = \hbar = k_B = \epsilon_0 = \mu_0 = 1$. The reduced Planck mass is defined as $m_P = (8\pi G)^{-1/2}$. We normalise the cosmic scale factor to unity today so that the comoving scales become physical scales today.

2. Axial coupling of electromagnetism to the inflaton

2.1. Action & field equations

We consider a scalar field, ϕ, which takes the role of the inflaton and the EM field, $F_{\mu\nu} \equiv \partial_\mu A_\nu - \partial_\nu A_\mu$, characterised by its four-vector potential A_μ. The EM field is conformally coupled to the metric and therefore, no fluctuations are generated unless there is either an explicit coupling to the inflaton or conformal symmetry is broken directly, e.g. by coupling F to a curvature term. Here, we investigate the first possibility and study a helical coupling given by the action

$$S[\phi, A_\mu] \equiv \int d^4x\sqrt{-g}\left\{Ł_\phi(\phi) + Ł_{\rm em}(A_\mu) + Ł_I(\phi, A_\mu)\right\} . \tag{1}$$

The Lagrangian densities of the free fields are

$$Ł_\phi(\phi) \equiv \frac{1}{2}g^{\alpha\beta}(\partial_\alpha\phi)(\partial_\beta\phi) + V(\phi) \tag{2}$$

$$Ł_{\rm em}(A_\mu) \equiv -\frac{1}{4}F_{\alpha\beta}F^{\alpha\beta} . \tag{3}$$

and the axial interaction is given by

$$Ł_I(\phi, A_\mu) \equiv \frac{1}{4}f(\phi)F_{\alpha\beta}\widetilde{F}^{\alpha\beta} . \tag{4}$$

It describes a coupling of the scalar field to the parity violating term, $F\widetilde{F}$, where $\widetilde{F}$ is the dual of the EM field tensor and is defined as

$$\widetilde{F}^{\mu\nu} \equiv \frac{1}{2}\eta^{\mu\nu\alpha\beta}F_{\alpha\beta} . \tag{5}$$

Here $\eta^{\mu\nu\alpha\beta}$ is the totally anti-symmetric tensor in four dimensions with $\eta^{0123} \equiv (-g)^{-1/2}$. For an observer with 4-velocity u_μ the electric and magnetic fields are $E_\mu = F_{\mu\alpha}u^\alpha$ and $B_\mu = \widetilde{F}_{\mu\alpha}u^\alpha$, respectively, and we have $F_{\alpha\beta}\widetilde{F}^{\alpha\beta} = -4E_\alpha B^\alpha$.

The axial coupling is characterised by the scalar function $f(\phi)$. We will see later how this function affects the evolution of the vector potential. Notice that if $f(\phi)$ was a constant, the EM part of the action would still be conformally invariant and therefore, no EM fluctuations could be amplified during inflation. Note also that the term $Ł_I$ either breaks parity explicitly if ϕ is a normal scalar field or, if ϕ is a pseudo-scaler, parity is broken spontaneously by the presence of a background field $\phi \not\equiv 0$. For the discussion in this work, this distinction is not relevant. However, in certain models, it might be relevant for the amount of parity violation generated during reheating.

Varying the action with respect to ϕ leads to a sourced equation of motion for the scalar field

$$\nabla^\alpha\partial_\alpha\phi - V'(\phi) = \frac{1}{4}f'(\phi)\,F_{\alpha\beta}\widetilde{F}^{\alpha\beta} . \tag{6}$$

The primes in $V'(\phi)$ and $f'(\phi)$ denote derivatives with respect to ϕ. The field equations for the EM field follow from varying the action with respect to A_μ:

$$\nabla_\alpha F^{\mu\alpha} = f'(\phi)\,(\partial_\alpha\phi)\,\widetilde{F}^{\mu\alpha} . \tag{7}$$

Comparison with the usual inhomogeneous Maxwell equation leads us to interpret the source term on the right hand side as an effective axial current‡. To obtain the above form of the inhomogeneous Maxwell equation, we used the homogeneous Maxwell equation

$$\nabla_\alpha \widetilde{F}^{\mu\alpha} \;=\; 0 \quad \Leftrightarrow \quad \nabla_{[\lambda} F_{\mu\nu]} \;=\; 0 \tag{8}$$

which is a consequence of the Bianchi identities, $dF = 0$.

2.2. Background evolution

To describe the universe during inflation, we work in a flat Friedmann-Lemaître (FL) background metric characterised by the line element

$$ds^2 \;=\; a^2(t)(-dt^2 + \delta_{ij}dx^i dx^j) \tag{9}$$

where a is the scale factor and t is conformal time which is related to cosmic time by $a\,dt = d\tau$. Derivatives with respect to conformal time are denoted by a dot and the conformal Hubble parameter is $\mathcal{H} \equiv \dot{a}/a = aH$ where $H \equiv (da/d\tau)/a$ is the physical Hubble parameter.

We assume the scalar field to dominate the energy budget of the universe and to drive inflation. We shall check later under what conditions the EM energy density is negligible and this approach is justified. We decompose the scalar field into a background value and a small perturbation: $\phi(x^\mu) \equiv \varphi(t) + \delta\phi(x^\mu)$. At background level, Eq. (6) reduces to the homogeneous evolution equation for the scalar field

$$\ddot{\varphi} + 2\,\mathcal{H}\dot{\varphi} + a^2 V'(\varphi) \;=\; 0\,. \tag{10}$$

The evolution of the scale factor is determined by the background Friedmann constraint equation

$$3\,m_P^2\mathcal{H}^2 \;=\; \frac{1}{2}\dot{\varphi}^2 + a^2 V(\varphi)\,. \tag{11}$$

During slow roll inflation, the potential of the inflaton field is dominating the energy density of the universe and the first term on the right hand side of Eq. (11) can be neglected. This is quantified by means of the slow roll parameters (see e.g. [34])

$$\epsilon \;\equiv\; \frac{m_P^2}{2}\left(\frac{V'}{V}\right)^2 \;\ll\; 1\,, \qquad \left|\frac{m_P^2}{3}\frac{V''}{V}\right| \;\ll\; 1\,. \tag{12}$$

To first order in the slow roll parameters, the evolution equation of φ and the Friedmann constraint can be reduced to [34]

$$\dot{\varphi} \;\simeq\; -\frac{a^2 V'}{3\mathcal{H}} \;=\; \pm\sqrt{2\epsilon}\,\frac{a^2 V}{3 m_P \mathcal{H}} \;\simeq\; \pm\sqrt{2\epsilon}\,m_P\mathcal{H}\,. \tag{13}$$

So far, we did not assume a specific form of the potential V. Now we assume that the inflaton is rolling down its potential from a large positive value so that $\dot{\varphi} < 0$. Using also that $\mathcal{H} \simeq |t|^{-1}$ during slow roll, we obtain

$$\dot{\varphi} \;\simeq\; -\sqrt{2\epsilon}\,m_P|t|^{-1}\,. \tag{14}$$

‡ An axial anomaly which also induces a source term of this form has been discussed in Ref. [33].

Since ϵ is nearly constant in the slow roll regime§, we can integrate this result to find

$$\varphi \;\simeq\; \varphi_{\rm in} + \sqrt{2\bar{\epsilon}}\, m_P \ln(t/t_{\rm in}) \tag{15}$$

where $\varphi_{\rm in} \equiv \varphi(t_{\rm in})$ is the initial value of the inflaton, and $\bar{\epsilon}$ is the average value of ϵ in the slow roll regime. However, in this approximation, any deviation from ϵ to be constant is integrated over time, which can lead to significant deviations in the evolution of φ towards the end of inflation.

For a given potential, we can obtain a better approximation for φ by inverting the definition of ϵ to find φ as a function of ϵ. Explicitly, for a power law potential we have

$$V \;=\; \frac{\lambda}{q} m_P^4 \left(\frac{\varphi}{m_P}\right)^q \quad \overset{(12)}{\Longrightarrow} \quad \varphi \;=\; \frac{q m_P}{\sqrt{2\epsilon}} \tag{16}$$

where we assume φ to be positive. This is an exact expression and can safely be approximated to be a constant in the slow roll regime, e.g. during horizon crossing of a given mode. Similar expressions can be found for any inflaton potential that admits a slow roll regime. We will use this result later when analytically studying the generation of magnetic fields in the slow roll approximation.

2.3. Linear perturbation equations

The EM field does not contribute to the background expansion but comes into play at the perturbative level. We study the generation of perturbations in the FL background during inflation. We work in longitudinal gauge where the metric perturbation is

$$\delta g_{\mu\nu} dx^\mu dx^\nu \;=\; a^2(t)\left(-2\Psi dt^2 - 2\Phi \delta_{ij} dx^i dx^j\right) \tag{17}$$

and the two scalar degrees of freedom, Ψ and Φ, coincide with the gauge-invariant Bardeen potentials [34].

We work in Coulomb gauge throughout, i.e. $A^\mu = (0, A^i)$ with $\partial_i A^i = 0$. To lowest order‖, the inhomogeneous Maxwell equation (7) with the axial current becomes

$$\ddot{A}_i - \nabla^2 A_i \;=\; -f'(\varphi)\dot{\varphi}\, \epsilon_{ijk} \partial_j A_k \,. \tag{18}$$

where the Euclidean Laplacian is defined as $\nabla^2 \equiv \delta^{ij}\partial_i\partial_j$ and the totally anti-symmetric symbol ϵ_{ijk} satisfies $\epsilon_{123} = 1$. Note that these equations are like in Minkowski space, there is no coupling to the scale factor. For a constant axial coupling, $f'(\varphi) = 0$, the sourced Maxwell equation reduces to the standard free wave equation and no fluctuations are amplified during inflation.

The evolution of perturbations in the scalar field is also altered by the axial coupling. At linear order, the scalar field equation (6) acquires a source term

$$\begin{aligned} \ddot{\delta\phi} + 2\mathcal{H}\dot{\delta\phi} - \nabla^2\delta\phi + a^2 V''(\varphi)\delta\phi - \dot{\varphi}(3\dot{\Phi} + \dot{\Psi}) + 2a^2 V'(\varphi)\Psi \\ = \; -a^{-2} f'(\varphi)\epsilon_{ijk}\dot{A}_i \partial_j A_k \,. \end{aligned} \tag{19}$$

§ To the first order in the slow roll parameters, ϵ is indeed a constant.

‖ Since the EM energy density is quadratic in the fields, one considers the vector potential and the electric and magnetic fields to be at half order in linear perturbation theory.

For any scenario where EM perturbations are generated, it is important to investigate the effect of this source term on the generation of scalar perturbations and through these on the primordial curvature perturbations. We leave the discussion of this effect for future work [35]. Here we concentrate on the generation of magnetic fields.

2.4. Physical properties of electromagnetism in the expanding universe

The four-vector potential is generally covariant and its evolution is independent of the choice of coordinates. However, for an observer, the physical EM field manifests itself in terms of electric and magnetic fields which are intrinsically frame dependent quantities. Measured by an observer with four-velocity u_μ, with $u^\alpha u_\alpha = -1$, the electric and magnetic fields can be covariantly defined as [36]

$$E_\mu \;=\; F_{\mu\alpha}u^\alpha \tag{20}$$

$$B_\mu \;=\; \frac{1}{2}\eta_{\mu\alpha\beta\gamma}F^{\alpha\beta}u^\gamma \;=\; \widetilde{F}_{\mu\alpha}u^\alpha\,. \tag{21}$$

These are both three-vector fields in the sense that they are orthogonal to the observer velocity, $E_\alpha u^\alpha = 0 = B_\alpha u^\alpha$. In a perturbed FL metric an observer has the four-velocity $u^\mu = a^{-1}(1,\mathbf{0}) + \mathcal{O}(1)$. As a consequence one finds

$$E_\mu \;=\; \Big(0,\; -\frac{1}{a}\dot{A}_i\Big)\,, \qquad B_\mu \;=\; \Big(0,\; \frac{1}{a}\epsilon_{ijk}\partial_j A_k\Big) \tag{22}$$

up to first order. With respect to an orthonormal basis comoving with the observer (or generally the Hubble flow), we define the Euclidean three-vector fields $\boldsymbol{E}$ and $\boldsymbol{B}$ through

$$E_\mu \;=\; a\Big(0,\; \boldsymbol{E}\Big)\,, \qquad B_\mu \;=\; a\Big(0,\; \boldsymbol{B}\Big)\,. \tag{23}$$

As discussed in Ref. [16], in a highly conducting plasma, magnetic fields should scale as a^{-2} with the expansion, while the electric field is damped away. The three-vector fields $\boldsymbol{E}$ and $\boldsymbol{B}$ defined above show exactly this property. We therefore rescale the fields by a factor of a^2 such that the effect of the expansion is absorbed, i.e. $\widetilde{\boldsymbol{B}} \equiv a^2\boldsymbol{B}$. In terms of the vector potential, the rescaled fields become

$$\widetilde{E}_i \;=\; -\dot{A}_i\,, \qquad \widetilde{B}_i \;=\; \epsilon_{ijk}\,\partial_j A_k\,. \tag{24}$$

Using these expressions and the field equations for A_μ, one can derive Maxwell's equations for the rescaled fields $\widetilde{\boldsymbol{E}}$ and $\widetilde{\boldsymbol{B}}$, which take the same form as in a Minkowski space-time.

The physical properties of the EM fields can now be described in terms of the rescaled fields. Here, we are mainly interested in the energy density and the helicity density of the fields generated during inflation. The energy density of the magnetic field is

$$\rho_B \;\equiv\; \frac{1}{2}B_\alpha B^\alpha \;=\; \frac{1}{2}\boldsymbol{B}\cdot\boldsymbol{B} \;=\; \frac{1}{2}a^{-4}\,\widetilde{\boldsymbol{B}}\cdot\widetilde{\boldsymbol{B}} \;\equiv\; a^{-4}\,\widetilde{\rho}_B \tag{25}$$

and analogously for the electric energy density. The helicity density is given as

$$\mathfrak{H} \;\equiv\; A_\alpha B^\alpha \;=\; a^{-3}\,\delta^{ij}A_i\widetilde{B}_j \;\equiv\; a^{-3}\,\widetilde{\mathfrak{H}}\,. \tag{26}$$

(Deliberately, we are not denoting the vector-potential in bold face because A_i are the spatial components of the four-vector A_μ in the covariant representation with respect to the metric, while e.g. $\boldsymbol{B}$ are the components of the four-vector B with respect to the orthonormal basis as discussed, for instance, in Ref. [16].)

3. Electromagnetic quantum fluctuations

To investigate the generation of EM fields during inflation, we consider the evolution of quantum fluctuations of the EM vector-potential. The coupling of the vector-potential to the background evolution of the inflaton via the inhomogeneous Maxwell equation (18) can lead to the amplification of EM quantum fluctuations. The amplification depends on the axial coupling $f(\varphi)$ and therefore on the evolution of φ. In Appendix A, we review the quantisation of the vector-potential in an expanding background. The result is that Maxwell's equations lead to an evolution equation for the Fourier modes of the quantised field which reduces to the free wave equation in the absence of the axial coupling. We first discuss this evolution equation and then summarise the physical observables of the EM field expressed in terms of the solutions to the mode equations.

3.1. Evolution of the Fourier modes of the vector potential

We introduce the orthonormal spatial basis as

$$\left(\boldsymbol{\varepsilon}_1^{\boldsymbol{k}}\,,\,\boldsymbol{\varepsilon}_2^{\boldsymbol{k}}\,,\,\hat{\boldsymbol{k}}\right) \qquad \text{with} \quad |\boldsymbol{\varepsilon}_i^{\boldsymbol{k}}|^2 = 1\,,\hat{\boldsymbol{k}} = \boldsymbol{k}/k\,, \tag{27}$$

and

$$\boldsymbol{\varepsilon}_\pm^{\boldsymbol{k}} \;\equiv\; \frac{1}{\sqrt{2}}\left(\boldsymbol{\varepsilon}_1^{\boldsymbol{k}} \pm i\boldsymbol{\varepsilon}_2^{\boldsymbol{k}}\right)\,. \tag{28}$$

In radiation gauge, the vector potential then takes the form

$$\boldsymbol{A} \;=\; \mathcal{A}_1\boldsymbol{\varepsilon}_1 + \mathcal{A}_2\boldsymbol{\varepsilon}_2 \;=\; \mathcal{A}_+\boldsymbol{\varepsilon}_+ + \mathcal{A}_-\boldsymbol{\varepsilon}_-\,. \tag{29}$$

After quantisation of the vector potential, we can study the evolution of the Fourier modes, $\mathcal{A}_h(t,k)$, with respect to the helicity basis for the polarisation states, $h = \pm$. We find that the helicity modes satisfy the wave equation with a time dependent mass term corresponding to the modified Maxwell equation (18) for the classical vector-potential,

$$\ddot{\mathcal{A}}_h + \left[k^2 + hkf'(\varphi)\dot{\varphi}\right]\mathcal{A}_h \;=\; 0\,. \tag{30}$$

The fact that the sign of the respective helicity mode, $h = \pm$, appears explicitly in the evolution equation of the Fourier modes, leads to a different evolution of the two helicity states and therefore, to the generation of magnetic helicity. Also note that the scalar field couples to $k\mathcal{A}_h$ and the coupling function itself, $f'(\varphi)\dot{\varphi}$, only depends on time, as φ is the background value of the inflaton. The solutions to this mode equation for a given coupling $f(\varphi)$ fully determines the spectrum of the generated EM fields.

Let us compare the mode equation (30) to the non-helical case with the coupling $f(\varphi)F^2$. One obtains a similar evolution equation [16]

$$\ddot{\mathcal{A}}_h + 2\frac{f'\dot{\varphi}}{f}\dot{\mathcal{A}}_h + k^2\mathcal{A}_h \;=\; 0\,. \tag{31}$$

Redefining the mode functions as $\bar{\mathcal{A}}_h \equiv f\mathcal{A}_h$, one can rewrite this in the form

$$\ddot{\bar{\mathcal{A}}}_h + \left[k^2 - \frac{\ddot{f}}{f}\right]\bar{\mathcal{A}}_h \;=\; 0\,. \tag{32}$$

We observe two significant differences to the helical case: firstly, the two helicity states couple with the same sign and therefore, no helicity is generated. Secondly, the scalar field couples to $\dot{\mathcal{A}}_h$ (or $\bar{\mathcal{A}}_h$) as opposed to $k\mathcal{A}_h$ in the helical case. As we shall see, this leads to significant differences in the spectra obtained for the two types of couplings. The reason is that the additional factor k in the helical case leads to a suppression of the coupling term at super-Hubble scales.

To visualise this, let us compare the importance of the different terms in the helical mode equation (30). We define f_N to be the logarithmic derivative of the coupling function, f, with respect to the scale factor

$$f_N \;\equiv\; \frac{df}{d\ln a} \;=\; \frac{f'(\varphi)\dot{\varphi}}{\mathcal{H}}\,. \tag{33}$$

where N stands for the number of e-foldings and is defined as $N = \ln(a/a_{\rm in})$. It turns out that f_N is the dimensionless part of the coupling term appearing in the mode equation (30). First consider super-Hubble scales, $k \ll \mathcal{H}$, where we can approximate $|\partial_t| \sim \mathcal{H}$ so that

$$\left[1 + \frac{k^2}{\mathcal{H}^2} + hf_N\frac{k}{\mathcal{H}}\right]\mathcal{A}_h \;\simeq\; 0\,. \tag{34}$$

The second term is small by definition and the coupling term can be important on super-Hubble scales only if f is a rapidly varying function of time, i.e. $f_N = \dot{f}/\mathcal{H} \gg 1$. However, if f_N is too large initially, it is impossible to define an appropriate initial vacuum as we shall see in the next section. Furthermore, such behaviour is constrained by the slow rolling of the inflaton and the possibility of a perturbative description of the system. Typically we rather expect $f_N \sim \mathcal{O}(1)$. On sub-Hubble scales, $k \gg \mathcal{H}$, we may approximate $\ddot{\mathcal{A}}_h \sim k^2\mathcal{A}_h$, because f is a background quantity and we still typically expect $f_N \sim \mathcal{O}(1)$, so that the first and second terms in Eq. (30) dominate. Hence the coupling term is typically relevant only at Hubble crossing $k \sim \mathcal{H}$ during a few Hubble times at best. In Fig. 1, we show the evolution of the two helicity modes for a given wavenumber in case of a power law coupling, $f \propto \varphi^p$. Clearly, the modes only feel the axial coupling around horizon crossing. This fact turns out to be relevant for the resulting spectrum. We will discuss this issue in more detail in Sec. 4.1.

3.2. Vacuum solutions & initial conditions

To study the generation of perturbations during inflation, we need to set the initial conditions when the mass term $\pm k\mathcal{H}f_N$ in Eq. (30) can be neglected, i.e. well inside

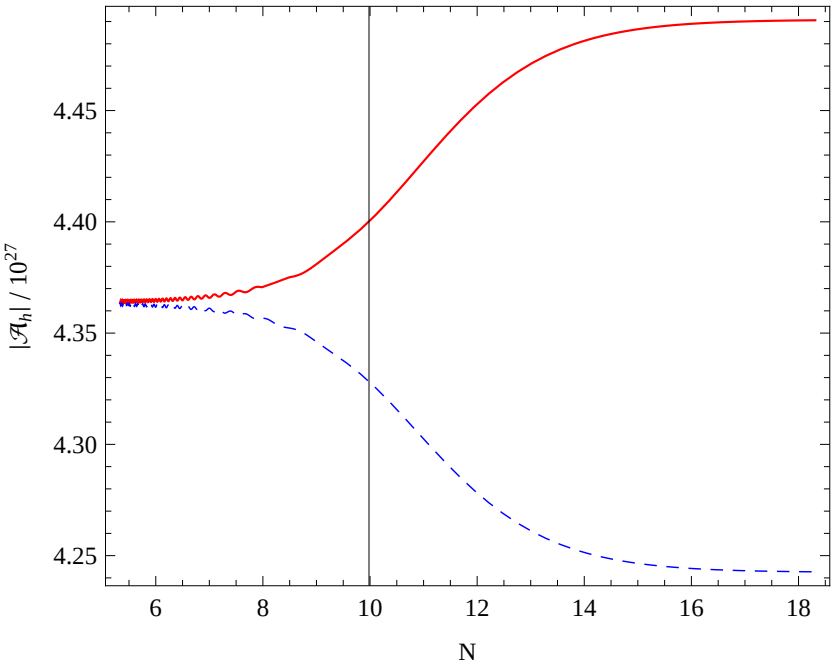

Figure 1. The evolution of the two helicity modes (+ solid red, − dashed blue) for wavenumber $k = 10/\mathrm{Mpc}$ is shown as a function of the number of e-foldings, N, during inflation. Here we consider an axial coupling function $f \propto \varphi^p$, as discussed in detail in Sec. 4.1. Both modes feel the axial coupling only around horizon crossing, at $N_{cross} \simeq 10$, while the evolution ceases and the modes saturate quickly after crossing. Note that here inflation ends at $N \simeq 60$.

the Hubble horizon at early times. This condition is usually formulated in terms of the variable $x \equiv -kt$ which approaches infinity in this limit. During slow roll inflation $\mathcal{H} \simeq -1/t$, so that $x = -kt \simeq k/\mathcal{H} \gg 1$ if the mode k is well inside the Hubble horizon.

From the mode equation (30), we see that if initially

$$f_N(\varphi_{\rm in}) \;=\; f'(\varphi_{\rm in})\dot{\varphi}_{\rm in}/\mathcal{H}_{\rm in} \;\ll\; k/\mathcal{H}_{\rm in} \tag{35}$$

the axial coupling term can be neglected with respect to the k^2 term and the mode equation becomes a free wave equation. Its solutions are plane waves. We match to the incoming vacuum solution described in Appendix A,

$$\mathcal{A}_h(t,k) \;= \mathcal{A}^{\rm free}(t,k) \;=\; (2k)^{-1/2} e^{-ikt}\,, \qquad \text{for} \quad -kt \gg 1\,. \tag{36}$$

This is used in the following as initial condition for the solutions of the full mode equation. Notice that the free plane wave solution only yields a valid initial condition if Eq. (35) is satisfied.

3.3. Power spectra & physical quantities

The statistical distribution of the EM fields as seen by an observer can now be quantified in terms of a given solution for the helicity modes of the EM vector potential. We define the magnetic power spectrum and relate it to the magnetic energy and helicity density.

If we assume that the magnetic field generated by some process is statistically homogeneous and isotropic, its spectrum is determined by two scalar functions $P_S(k)$ and $P_A(k)$. Since the magnetic field is a divergence-free vector field the two-point function of the Fourier components of the magnetic field can therefore be written as

$$\langle \widetilde{B}_i(t,\boldsymbol{k})\widetilde{B}_j^*(t,\boldsymbol{q})\rangle = \frac{(2\pi)^3}{2}\delta(\boldsymbol{k}-\boldsymbol{q})\Big\{(\delta_{ij}-\hat{k}_i\hat{k}_j)P_S(t,k) - i\epsilon_{ijn}\hat{k}_n P_A(t,k)\Big\} \tag{37}$$

where P_S and P_A are the symmetric and anti-symmetric parts of the power spectrum, respectively. The symmetric part of the spectrum determines the energy density while the anti-symmetric part corresponds to the helicity density:

$$\langle \widetilde{B}_i(t,\boldsymbol{k})\widetilde{B}_i^*(t,\boldsymbol{q})\rangle = (2\pi)^3\delta(\boldsymbol{k}-\boldsymbol{q})P_S(t,k) \tag{38}$$

$$\begin{aligned}\langle \widetilde{A}_i(t,\boldsymbol{k})\widetilde{B}_i^*(t,\boldsymbol{q})\rangle &= ik^{-2}\langle(\boldsymbol{k}\wedge\widetilde{\boldsymbol{B}})_i(t,\boldsymbol{k})\widetilde{B}_i^*(t,\boldsymbol{q})\rangle \\ &= k^{-1}(2\pi)^3\delta(\boldsymbol{k}-\boldsymbol{q})P_A(t,k)\,.\end{aligned} \tag{39}$$

With respect to the helicity basis, see Appendix A, the spectra can directly be written as

$$P_{S/A}(t,k) = k^2\left(|\mathcal{A}_+(t,k)|^2 \pm |\mathcal{A}_-(t,k)|^2\right)\,, \tag{40}$$

where the upper sign corresponds to P_S and the lower sign to P_A. Here we use the non-trivial result widely applied in inflationary cosmology that at late times, the vacuum expectation values of the fields generated during inflation can be interpreted as stochastic power spectra. We define the magnetic energy density per logarithmic wave number via

$$\langle\widetilde{\rho}_B(t)\rangle = \int_0^\infty \frac{dk}{k}\,\frac{d\widetilde{\rho}_B}{d\ln k}(t,k)\,, \tag{41}$$

so that

$$\frac{d\widetilde{\rho}_B}{d\ln k}(t,k) = \frac{k^3}{(2\pi)^2}P_S(t,k)\,. \tag{42}$$

Similarly, we define the magnetic helicity per logarithmic wave number as $\widetilde{\mathfrak{H}} = A_\alpha\widetilde{B}^\beta$,

$$\frac{d\widetilde{\mathfrak{H}}}{d\ln k}(t,k) = \frac{k^2}{2\pi^2}P_A(t,k)\,. \tag{43}$$

Finally, the electric field is given by the time derivative of the vector-potential and thus its contribution to the energy density, $\widetilde{\rho}_E = \widetilde{E}_\alpha\widetilde{E}^\alpha/2$, is computed to be

$$\frac{d\widetilde{\rho}_E}{d\ln k}(t,k) = \frac{k^3}{(2\pi)^2}\left(|\dot{\mathcal{A}}_+(t,k)|^2 + |\dot{\mathcal{A}}_-(t,k)|^2\right)\,. \tag{44}$$

Notice that any electric fields produced during inflation will be diffused very rapidly after inflation due to the huge conductivity of the primordial plasma.

4. Analytic solutions during slow roll inflation

We turn to solving the vector-potential mode equation (30) for particular cases and discuss why we expect the result to hold for any reasonable axial coupling of the inflaton to the EM field as long as the slow roll approximation is assumed.

4.1. Power law coupling

We first study the special case of a power law coupling,

$$f(\varphi) \;=\; f_0 \Big(\frac{\varphi}{m_P}\Big)^p . \tag{45}$$

Here f_0 and p are constants. The sign of f_0 determines which helicity is amplified by the coupling and, thus, we can take f_0 to be positive without loss of generality. Let us first investigate bounds on the parameter space of f_0 and p before investigating the coupling term f_N of the mode equation in the slow roll approximation.

For perturbation theory to be valid and the coupling not to become too strong, one has to require $|f(\varphi)| \leq 1$ for all values φ takes during inflation. This condition can be turned into an upper bound on f_0 depending on p:

$$f_0^{max} \;\equiv\; \min_{\varphi} \left(\frac{m_P}{\varphi}\right)^p \;=\; \begin{cases} (m_P/\varphi_{\rm in})^p & \text{if } p > 0 \\ (m_P/\varphi_{\rm end})^p & \text{if } p \leq 0\,. \end{cases} \tag{46}$$

To arrive at these bounds, we used the fact that, typically the inflaton takes its largest value at the beginning of inflation, $\varphi_{\rm in}$, while it is smallest at the end of inflation, $\varphi_{\rm end}$. This upper bound on f_0 leads to a stringent limitation of the magnetic field generation if φ is not changing rapidly.

During slow roll inflation, we use Eqs. (14) and (16) to express the coupling term in the mode equation (30), $f_N = f'(\varphi)\dot{\varphi}/\mathcal{H}$, in terms of the slow roll parameter ϵ. For a power law inflaton potential, $V(\varphi) \propto \varphi^q$, we find

$$f_N \;\simeq\; -f_0\, p\, q^{p-1}\, (2\epsilon)^{1-p/2} \tag{47}$$

where, in principle, ϵ is a slowly varying function of time. Typically it is slowly increasing from its initial value and stays small in the slow roll regime, $\epsilon_{\rm in} \lesssim \epsilon \ll 1$, before reaching unity at the end of inflation, $\epsilon_{\rm end} = 1$. As we mention earlier, well in the slow roll regime, ϵ can be considered approximately constant. We investigate the behaviour of the coupling term f_N in terms of the maximal absolute value as a function of p and ϵ:

$$f_N^{max} \;\equiv\; |f_N(f_0^{max}, p, \epsilon)| \;\simeq\; \begin{cases} 2\, p\, q^{-1}\, \epsilon\, (\epsilon_{\rm in}/\epsilon)^{p/2} & \text{if } p > 0 \\ 2\, |p|\, q^{-1}\, \epsilon^{1+|p|/2} & \text{if } p \leq 0\,. \end{cases} \tag{48}$$

For fixed ϵ as a function of p, f_N^{max} increases as $|p|$ before it is suppressed by $\epsilon^{1+|p|/2}$ for negative p. For positive p, it also increases as p but is suppressed more slowly by $\epsilon(\epsilon_{\rm in}/\epsilon)^{p/2}$. We visualise this behaviour in Fig. 2 where we plot f_N^{max} as a function of p for typical values of ϵ and $\epsilon_{\rm in}$. Most importantly, we find that in all cases $f_N^{max} \ll 1$.

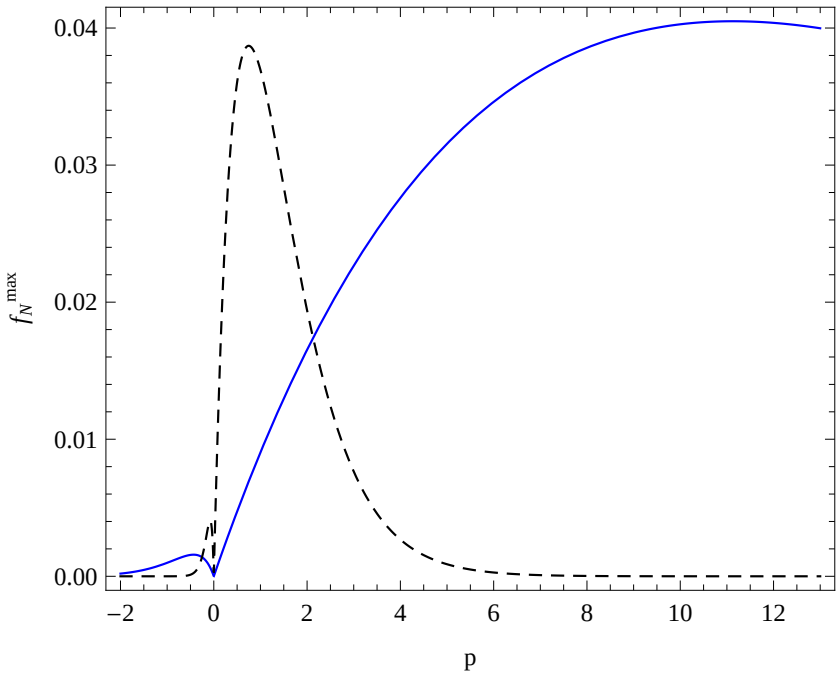

Figure 2. We investigate possible values of the axial coupling term, $f_N = f'(\varphi)\dot{\varphi}/\mathcal{H}$, in the slow roll regime. We plot the maximal possible value, $f_N^{max}(p) \equiv |f_N(f_0^{max}, p)|$, as a function of p for a fixed typical value of ϵ. We compare the power law case, $f \propto \varphi^p$, discussed in this section (blue solid), with the exponential model, $f \propto \exp(p\varphi)$, discussed in the next section (black dashed). For the slow roll parameter we use the values from our numerical study in Sec. 5: for $q = 2$ we have $\epsilon_{\rm in} \simeq 0.008$ initially and $\epsilon_k \simeq 0.01$ at Hubble crossing of $k = 10/\text{Mpc}$. For the power law, f_N^{max} takes its maximal value, $f_N^{max}(p_k^{\max}) \simeq 0.04$ at $p_k^{max} \simeq 11$. We confirm that in any case $f_N^{max} \ll 1$.

This can be verified by looking at the maximum of $f_N^{max}(p)$ for a given ϵ_k, which can be thought of as the epoch during slow roll inflation at which a certain scale of interest crosses the Hubble scale, $k = \mathcal{H}(\epsilon_k)$. The coupling f_N is maximal for $p_k^{\max} = 2/\ln(\epsilon_k/\epsilon_{\rm in})$, assuming $p > 0$, where it takes the value

$$f_N^{max}(p_k^{\max}) \;\simeq\; \frac{4}{e\,q}\,\frac{\epsilon_k}{\ln(\epsilon_k/\epsilon_{\rm in})}\,. \tag{49}$$

Here, $e \simeq \exp(1) \simeq 2.72$ is Euler's number and we remind the reader that $q \geq 2$ is the power of the inflaton potential in consideration. Since $\epsilon_{\rm in} < \epsilon_k \ll 1$, the coupling term is always < 1. This reasoning is not valid for the limit $\epsilon_k \to \epsilon_{\rm in}$, where p could be chosen arbitrarily large while f_0 would become arbitrarily small.

Firstly, we conclude that the condition that $|f(\varphi)| \leq 1$ at any time during inflation, restricts the parameter space of f_0 and p in such a way that the coupling term, f_N, remains small throughout the slow roll regime for a typical inflation model. Secondly, because $f_N \propto (2\epsilon)^{1-p/2}$, the coupling term is approximately constant all through slow roll inflation for any possible values of p and f_0. As we shall argue below, this conclusion is not only valid for power law couplings but also for any other reasonable form of coupling

and of the inflaton potential.

We can now solve the mode equation (30) for this coupling. Since f_N is approximately constant in the slow roll regime, the full coupling term is, $f'(\varphi)\dot{\varphi} = f_N\mathcal{H} \simeq -f_N/t$, i.e. inversely proportional to conformal time and, consequently, the mode equation can be solved analytically. It is convenient to use $x \equiv -kt$ as the time evolution variable. For each scale, k, the initial condition in the asymptotic past is set well inside the horizon, i.e. for $x \to \infty$, while inflation is considered to end when $x \to 0$. With a prime denoting the derivative with respect to x, the mode equation reads

$$\mathcal{A}_h''(x) + \left(1 + hf_N x^{-1}\right)\mathcal{A}_h(x) \;=\; 0\,. \tag{50}$$

Since $|f_N| < 1$, the free solution is a good approximation at early times, $x \gg 1$. The general solution to the mode equation (50) is [37]

$$\mathcal{A}_h(x) \;=\; C_1 G_0(y,x) + C_2 F_0(y,x) \tag{51}$$

where $y \equiv -hf_N/2$ and G_0 and F_0 are the irregular and regular Coulomb wave functions of order zero, respectively. As initial condition we require the solution to approach the free solution, Eq. (36), for $x \to \infty$. It turns out that the combination $G_0 \pm iF_0$ has the desired limit, as given in Ref. [37]:

$$G_0(y,x) \pm iF_0(y,x) \underset{x\to\infty}{\longrightarrow} \exp \pm i\left[x - y\ln(2x) + \sigma_0(y)\right] \tag{52}$$

with $\sigma_0(y) \equiv \arg\Gamma(1+iy) = \gamma_E y + \mathcal{O}(y^3)$ and $\gamma_E \simeq 0.58$ being the Euler's constant. Because $|y| = f_N/2 < 1$, as discussed above, the second term in the exponential, $y\ln(2x)$, can be neglected with respect to x. Comparison with the free solution shows that the plus sign corresponds to the incoming vacuum solution and we have to choose the initial amplitude

$$\frac{1}{2}(C_1 - iC_2) \;=\; (2k)^{-1/2} \quad \text{and} \qquad \frac{1}{2}(C_1 + iC_2) \;=\; 0\,. \tag{53}$$

The factor with σ_0 only acts as an overall phase and has no physical significance. The normalised full solutions are

$$\mathcal{A}_h(x) \;=\; (2k)^{-1/2}\left[G_0(-hf_N/2,x) + iF_0(-hf_N/2,x)\right] \tag{54}$$

for $h = \pm 1$. This solution of the mode equation has also been found in Ref. [31] for N-flation. Below we shall argue that it is very general.

To understand the effect of the axial coupling on the growth of EM quantum fluctuations and to compute the magnetic power spectra at the end of inflation, we analyse the late time limit of this solution, i.e. when $x \to 0$. Using the approximate expressions derived in Appendix B, we find the asymptotic limit at late times as

$$\mathcal{A}_h(x) \underset{x\to 0}{\longrightarrow} (2k)^{-1/2}\left[\frac{\exp(-h\pi f_N/2)\sinh(\pi f_N/2)}{\pi f_N/2}\right]^{1/2}. \tag{55}$$

The late time behaviour of both helicity modes is independent of x, and therefore of t, and the scale-dependence is not changed with respect to the free solution. The modes are coherently amplified while crossing the horizon, before they saturate outside the

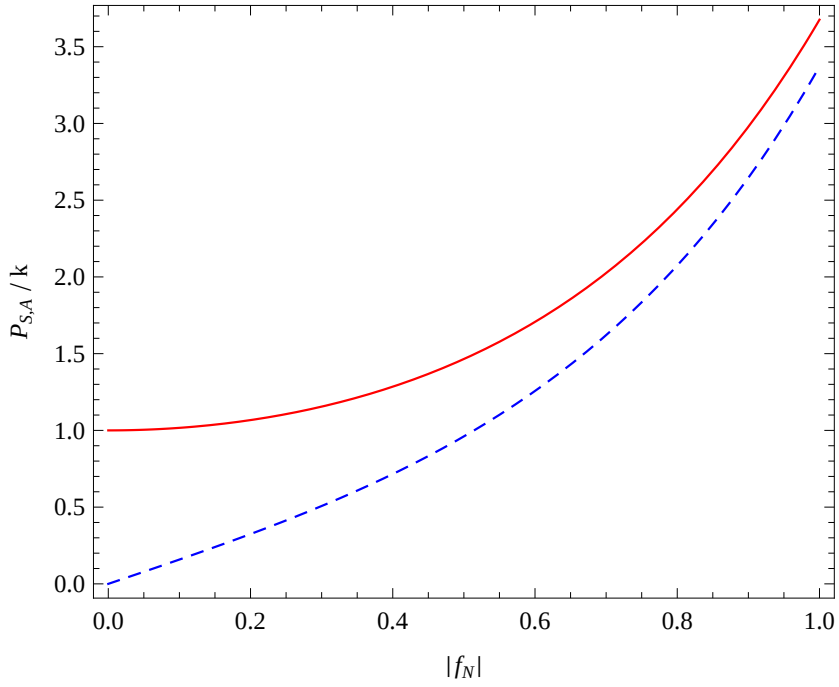

Figure 3. The symmetric and antisymmetric power spectra of the magnetic fields, $P_{S,A}/k$, are plotted as a function of the effective coupling constant $|f_N|$. For vanishing coupling, the vacuum solution, $P_S/k = 1$ and $P_A/k = 0$ is recovered, while the larger the coupling, the smaller the difference between P_S and P_A. As discussed in the main text, typically $|f_N| \ll 1$ and therefore, the amplification of the magnetic fields is small.

horizon. Notice also that we did not use the asymptotic limit given in 14.6.9-10 of Ref. [37] because it is not correct. (In this context, see discussion in Appendix B.)

Given the late time behaviour of the helicity mode functions, it is easy to compute the magnetic field power spectra produced at the end of inflation. The symmetric power spectrum is

$$P_S(k) \;=\; k\,\frac{\sinh(\pi f_N)}{\pi f_N} \;\simeq\; k\left[1+\frac{(\pi f_N)^2}{6}\right] \tag{56}$$

while the antisymmetric one is

$$P_A(k) \;=\; k\,\frac{\cosh(\pi f_N)-1}{\pi f_N} \;\simeq\; k\,\frac{\pi f_N}{2}\,. \tag{57}$$

Here the last $\simeq$ sign is valid for $\pi f_N \ll 1$. Notice that both spectra are proportional to k and only their amplitude changes with the coupling strength f_N. In Fig. 3, we illustrate the k-independent amplification factors of P_S and P_A as a function of f_N. The larger $|f_N|$ the smaller the difference between P_S and P_A, i.e. the more helical the magnetic fields become. As one infers from Eqs. (56) and (57), both amplification factors tend to $(2\pi f_N)^{-1}\exp(\pi f_N)$ for large values of f_N.

The magnetic energy density per logarithmic wave number at the end of inflation can directly be computed to be

$$\frac{d\rho_B}{d\ln k}(t_{\rm end},k) \;=\; a_{\rm end}^{-4}\frac{d\widetilde{\rho}_B}{d\ln k}(t_{\rm end},k) \;=\; \frac{k^4}{a_{\rm end}^4}\,\frac{\sinh(\pi f_N)}{4\pi^3 f_N} \\ \equiv\; \frac{k^4}{a_{\rm end}^4}\,\mathcal{S}^2(f_N)\,. \tag{58}$$

Here, we define $\mathcal{S}(f_N)$ to be the amplitude of magnetic energy density spectrum. Since its spectrum is blue, the magnetic energy density is dominated by the cut-off scale, which is set by the last scale that exits the horizon before the end of inflation, $k_c = \mathcal{H}_{\rm end} = (aH)_{\rm end}$. Since $|f_N| < 1$ in the slow roll regime, one can therefore estimate that

$$\rho_B(t_{\rm end}) \;\simeq\; \frac{1}{4}H_{\rm end}^4\,\mathcal{S}^2(f_N)\,. \tag{59}$$

By means of the Friedmann equation, we have

$$\Omega_B(t_{\rm end}) \;\equiv\; \frac{\rho_B}{\rho_{\rm tot}} \;\simeq\; \frac{\mathcal{S}^2(f_N)}{12}\left(\frac{H_{\rm end}}{m_P}\right)^2 \tag{60}$$

and as we found that for typical couplings, $\mathcal{S}(f_N)$ is of order unity and therefore, no back-reaction on the background evolution is expected if inflation ends well below the Planck scale.

At the end of inflation and after reheating, we expect the universe to be filled with relativistic standard model particles. This makes up a relativistic highly conducting plasma. In this medium, the MHD approximation is valid and electric fields are rapidly damped away. We therefore do not discuss the electric field spectrum which will not survive reheating.

The helicity density per logarithmic wave number at the end of inflation is simply given by

$$\frac{d\mathfrak{H}}{d\ln k}(t_{\rm end},k) \;=\; \frac{k^3}{a_{\rm end}^3}\,\frac{\cosh(\pi f_N)-1}{2\pi^3 f_N}\,. \tag{61}$$

Note that $\widetilde{\mathfrak{H}} \propto \widetilde{\rho}_B/k_c$, which therefore has to be constant when helicity is conserved.

In principle we have to evaluate f_N at horizon crossing, $\epsilon = \epsilon_k$, which leads to a slight modification in the spectrum. In the following we neglect this effect, as it is quite irrelevant for the few orders of magnitude in k which we are interested in, see Fig. 5.

4.2. Exponential coupling

As a second case, we study the example of an exponential chiral coupling of the following form

$$f(\varphi) \;=\; f_0\,e^{\alpha(\varphi/m_P)} \tag{62}$$

where f_0 and α are constants. We could hope to obtain a different spectrum in this case. The reason for this is as follows: if we insert the solution (15) for φ and (14) for $\dot{\varphi}$ for the coupling term f_N, we obtain

$$f_N \simeq \; -f_0\,\alpha\,\sqrt{2\epsilon}\,e^{\alpha(\varphi_{\rm in}/m_P)}\left(\frac{t}{t_{\rm in}}\right)^{\alpha\sqrt{2\epsilon}} \; . \tag{63}$$

In this case, the full coupling term $f'(\varphi)\dot{\varphi}$ in the mode equation (30) explicitly depends on the conformal time as $t^{-1+\alpha\sqrt{2\epsilon}}$ and could therefore lead to more interesting solutions as in the case discussed above. For example, if $\alpha\sqrt{2\epsilon} = -1$, the solutions to the mode equation are Bessel functions and the spectral index turns out to depend on the pre-factor of the coupling term. However, using typical values for slow roll inflation, $\varphi_{\rm in} \gtrsim 10\,m_P$, $\bar{\epsilon} = 0.01$, the pre-factor becomes tiny, $f_0\,e^{\alpha(\varphi_{\rm in}/m_P)} \lesssim f_0 10^{-30}$. For a consistent treatment of this term during the entire period of inflation, also at the end when $\varphi \sim m_P$, we must require $|f_0| < 10$. Hence for such a value of α, the coupling remains totally negligible during the entire period of slow roll inflation. It can become relevant only towards the end of inflation when very small scales can still become amplified. See Fig. 2 for a study of the coupling f_N for this case compared to the power law coupling.

After inflation, when a plasma containing charged relativistic particles is present, such small scale magnetic fields are rapidly damped and therefore, they are uninteresting for cosmology.

We believe that this result is more general than the case studied here: whenever the function f is rapidly varying so that $f(\varphi) =$ constant during slow roll is no longer a good approximation, the fact that we have to require $|f(\varphi)| < 1$ during the entire period of inflation will render it so small during the phase of interest, when cosmologically relevant scales exit the Hubble horizon, that no significant amplification of vacuum fluctuations takes place. We have checked this statement numerically using different forms of exponential coupling terms. We, therefore, conclude that as long as the slow roll approximation is valid, the amplification of helical magnetic fields is always mode independent and consequently leads to a $n = 1$ spectrum for both the magnetic field and the helicity.

Note that this result differs significantly from the non-helical case. There, the source term in the mode equation is of the form $\ddot{f}/f$ which is typically $\propto 1/t^2$. The solutions are then Bessel functions and the Bessel function index, which determines the spectral index at late times is related to the (nearly arbitrary) pre-factor. The difference comes from the fact that a term of order $1/t^2$ is relevant during all the time when the mode is super-Hubble, $-kt < 1$, while a term of order $(k/t)\mathcal{A}_h$ is relevant only around horizon crossing. On super-Hubble scales, it is dominated by the $\ddot{\mathcal{A}}_h \sim \mathcal{A}_h/t^2$ term while on sub-Hubble scales, the $k^2\mathcal{A}_h$ term becomes dominant.

5. The effects of deviations from slow roll

In the previous section, we discuss two different functional forms of the axial coupling of the inflaton to the EM field, namely a power law and an exponential. Within the slow roll approximation, we find that the restriction that the coupling be small, $|f(\varphi)| \leq 1$, always leads to a magnetic field power spectrum proportional to k. In this section, we first confirm our analytical findings numerically. Second, we explore the possibility of obtaining a different magnetic field spectrum by introducing a short deviation from slow roll, motivated by the fact that such deviations can provide considerably better fit to the angular power spectrum of the CMB anisotropies than the predictions from typical single field inflation models, see for instance Refs. [38, 39, 40, 41, 42, 43].

To compare the analytical result, Eq. (56), to a full numerical solution, we solve the background evolution of φ with a quadratic potential, $V_0(\varphi) \equiv \frac{1}{2}m^2\varphi^2$, and integrate the evolution of the modes $\mathcal{A}_h(t,k)$ to compute the magnetic power spectrum $P_S(k)$ at the end of inflation.

A short deviation from slow roll can, for example, be achieved by introducing a

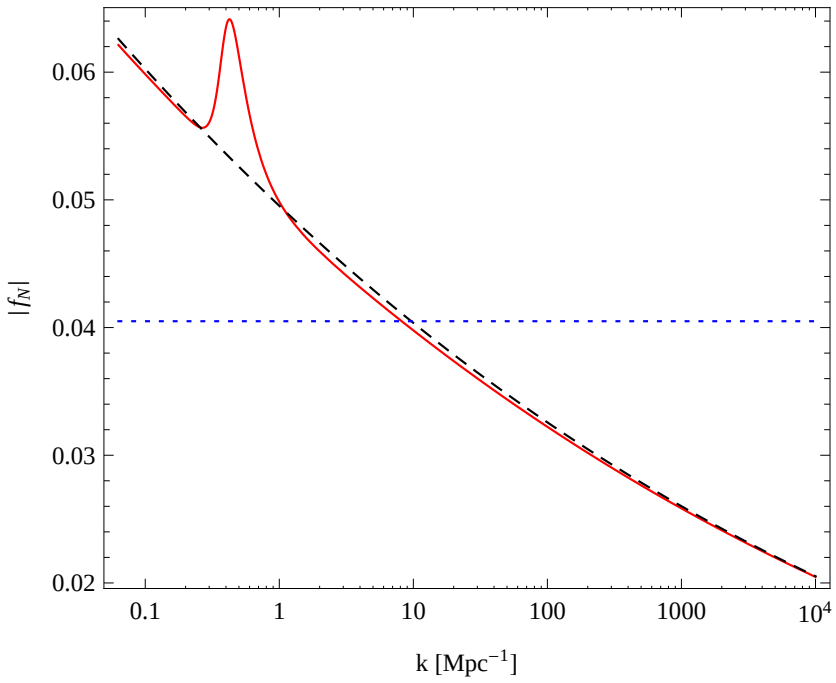

Figure 4. The coupling term $|f_N|$ at Hubble crossing of the wave number k is plotted for the power law coupling with positive power p. The horizontal dotted blue line indicates the maximal value of $|f_N|$ in the slow roll approximation optimised at wavenumber $k = 10/\text{Mpc}$. Optimised at the same scale, the dashed black line indicates the behaviour of the coupling term for the potential in Eq. (64) with $\beta = 0$, while the solid red line represents the same for $\beta \neq 0$. For the later case, we have used the best fit values of the parameters of the potential as in Ref. [43]. The bump in the coupling term for $\beta \neq 0$ arises due to the short period of deviation from slow roll.

step in the quadratic inflaton potential as follows [38, 39, 40, 44]

$$V_\beta(\varphi) \;=\; \frac{1}{2}m^2\varphi^2\left[1+\beta\tanh\left(\frac{\varphi-\varphi_0}{\Delta\varphi}\right)\right]. \tag{64}$$

Here β, φ_0 and $\Delta\varphi$ characterise the height, the location and the width of the step, respectively. Such a deviation from slow roll, in general, leads to a burst of oscillations in the primordial power spectrum of curvature perturbations. In what follows, we turn our attention to the possible effects of such a deviation from slow roll on the magnetic field power spectrum.

As we discuss earlier, the coupling term f_N is typically relevant only around Hubble crossing for a few Hubble times. In order to maximise the coupling term, we use the bounds on f_0 obtained in the previous section and also the maximum value of the index p evaluated at wavenumber $k = 10/\mathrm{Mpc}$, see Eq. (49). The coupling term is, in general, a function of time but this time dependence can be translated into a scale dependence by identifying a time with the corresponding Hubble crossing scale, $k = \mathcal{H}(\epsilon_k)$. In

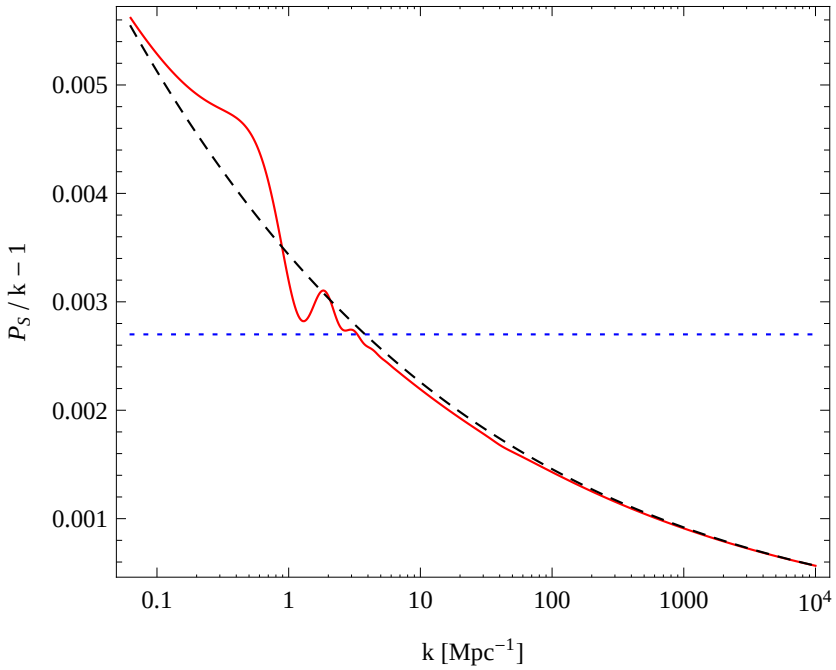

Figure 5. The relative deviation of the magnetic field power spectrum from an exact k-spectrum is plotted as a function of the wave number k for power law coupling with positive values of p. The dashed black line indicates the numerical solution for slow roll inflation ($\beta = 0$) while the solid red line is the spectrum resulting from a deviation from slow roll. The horizontal dotted blue line is the magnetic field spectrum from the slow roll approximation, $f_N = \text{const.}$, corresponding to the maximum value of f_N. The deviation from this approximated spectrum is always less than 1/2%. Only the scales which exit the Hubble radius around the time when a deviation from slow roll *or* equivalently a bump in the coupling term occurs are affected. This leads to small modulations in the spectrum over an exact k-spectrum.

Fig. 4 we plot the coupling term f_N at Hubble crossing of the mode k for the power law coupling with $p > 0$. It is evident from the figure that a deviation from slow roll leads to small bump in the coupling term as compared to the slow roll case and therefore, one can expect an effect in the magnetic field power spectrum on the scales which exit the Hubble radius around the time when the bump in the coupling term appears.

In Fig. 5, we plot the relative deviation of the magnetic field power spectrum over an exact k-spectrum as a function of k for the power law coupling. The exact numerical solution for slow roll deviates slightly from the $P_s \propto k$ spectrum due to the slight scale dependence of $\mathcal{S}^2(f_N)$. Small modulations in the spectrum arise as a result of a deviation from slow roll. We find that for the best fit values of the parameters of the potential (64), the spectrum of the magnetic field is not strongly modified. Indeed, we conclude that even the deviation from slow roll, within the limits required by CMB data, does not significantly modify the magnetic field spectrum. We find that the exponential coupling leads to a similar behaviour for the coupling term and the magnetic field spectrum.

6. Magnetic field at the end of inflation and its further evolution

Our main results are Eqs. (58) and (61) which determine the magnetic energy density and helicity density at the end of inflation. Note, however, that we do not renormalise the energy density. Hence even for $f_N = 0$, we obtain the non-vanishing result

$$\frac{d\widetilde{\rho}_B}{d\ln k}(t_{\rm end}, k) \;=\; \frac{k^4}{(2\pi)^2}$$

which comes purely from (not amplified) vacuum fluctuations and may be unphysical. However, from Eq. (40) it is clear that $P_S(k) \leq |P_A(k)|$ by definition. Hence the physical result cannot be obtained by a simple subtraction of the vacuum contribution as then $P_S \propto {f_N}^2$ would become smaller than $P_A \propto f_N$ for small values of f_N, see Eqs. (56) and (57). On the other hand, for $f_N \gtrsim 1$, the vacuum contribution becomes subdominant and it is no longer important to subtract it. We shall therefore not perform any renormalisation of the magnetic energy density but just keep in mind that our result becomes dominated by vacuum fluctuations in the limit $f_N \to 0$.

After inflation, the thermal cosmic plasma contains many relativistic charged particles and can be treated as an MHD plasma. During the process of reheating, the Reynolds number becomes very high and MHD turbulence develops. In the MHD limit the electric field is damped away and the magnetic field evolves by two different processes: it is damped on small scales and it undergoes an inverse cascade due to helicity conservation [20]. Numerical studies have shown that very soon damping on small scales leads to a maximally helical field (for which either $\mathcal{A}_+$ or $\mathcal{A}_-$ vanishes) which then continues to evolve via an inverse cascade, see [21, 22]. The inverse cascade is active as long as the Reynolds number of the cosmic fluid at the scale under consideration is larger than one and the fluid is therefore turbulent [45]. The damping scale $k_{\rm diss}(t)$ is the scale at which the Reynolds number becomes of order unity. On scales smaller than

$k_{\rm diss}(t)$ the magnetic field and the turbulent motion of the fluid decay exponentially by viscosity damping.

In the following we investigate how the spectrum of helical magnetic fields evolves during the turbulent epoch. We first discuss the evolution of the correlation scale of the magnetic field and the duration of the turbulent phase, before computing the magnetic energy spectrum at the end of the inverse cascade. Here we assume that the reheating epoch is relatively short and ends at t_*. This corresponds to the reheating temperature T_*, and because of radiation domination, we can approximately use $t/t_* \simeq T_*/T$ during the turbulent phase.

The helical magnetic field from inflation always has a blue spectrum and is therefore dominated by the largest wavenumber crossing the Hubble scale at the end of inflation or, for simplicity, reheating

$$\widetilde{\rho}_B(t_*, k_*) \;\simeq\; k_*^4\, \mathcal{S}^2(f_N)\,, \qquad \text{with} \quad k_* \simeq \mathcal{H}_*\,.$$

Accordingly, the correlation scale (which is roughly given by the scale at which the power spectrum peaks) is initially $k_c(t_*) = k_*$. As an example we consider $T_* = 10^{14}\,\text{GeV}$ and find

$$\begin{aligned} k_c(t_*) \;&=\; k_* \;=\; \mathcal{H}_* \;=\; H_* a_* \;=\; \sqrt{\frac{a_{SB}}{3}}\, g_0^{1/3} g_*^{1/6} \frac{T_0}{m_P} T_* \\ &\simeq\; 10^{-17}\,\text{GeV} \left(\frac{g_*}{200}\right)^{1/6} \left(\frac{T_*}{10^{14}\,\text{GeV}}\right) \\ &\simeq\; 2\times 10^{21}\,\text{Mpc}^{-1} \left(\frac{g_*}{200}\right)^{1/6} \left(\frac{T_*}{10^{14}\,\text{GeV}}\right)\,. \end{aligned} \tag{65}$$

Here a_{SB} is the Stefan-Boltzmann constant, $a_{SB} = \pi^2/15$ in our units, g_* and $g_0 = 2$ denote the number of relativistic degrees of freedom at t_* and today, respectively, and $T_0 = 2.73\,\text{K}$ is the present CMB temperature.

Let us assume that the inverse cascade starts at t_*. In Ref. [22] it was found that during the inverse cascade of a maximally helical magnetic field the total rescaled energy density scales like

$$\widetilde{\rho}_B(t) \;\propto\; (t/t_*)^{-2/3}$$

and the comoving correlation scalce evolves in the same way

$$k_c(t) \;=\; k_c(t_*)\,(t/t_*)^{-2/3}$$

such that the ratio $\widetilde{\rho}_B/k_c$ which is proportional to the helicity remains constant. This continues until $t_{\rm fin}$, the time when the damping scale has grown up to the correlation scale, $k_{\rm diss}(t_{\rm fin}) = k_c(t_{\rm fin})$. After $t_{\rm fin}$ the inverse cascade and turbulence cease and the magnetic field evolves solely by flux conservation on large scales

$$\frac{d\widetilde{\rho}_B}{d\ln k}(k,t) \;=\; \frac{d\widetilde{\rho}_B}{d\ln k}(k,t_{\rm fin}) \qquad \text{for} \quad t > t_{\rm fin}\,,\; k < k_{\rm diss}(t)$$

and viscosity damping on small scales, $k > k_{\rm diss}(t)$. At the end of the inverse cascade, the correlation scale of magnetic field spectrum has moved to

$$k_{\rm fin} \;\equiv\; k_c(t_{\rm fin}) \;=\; k_*\,(T_{\rm fin}/T_*)^{2/3}$$

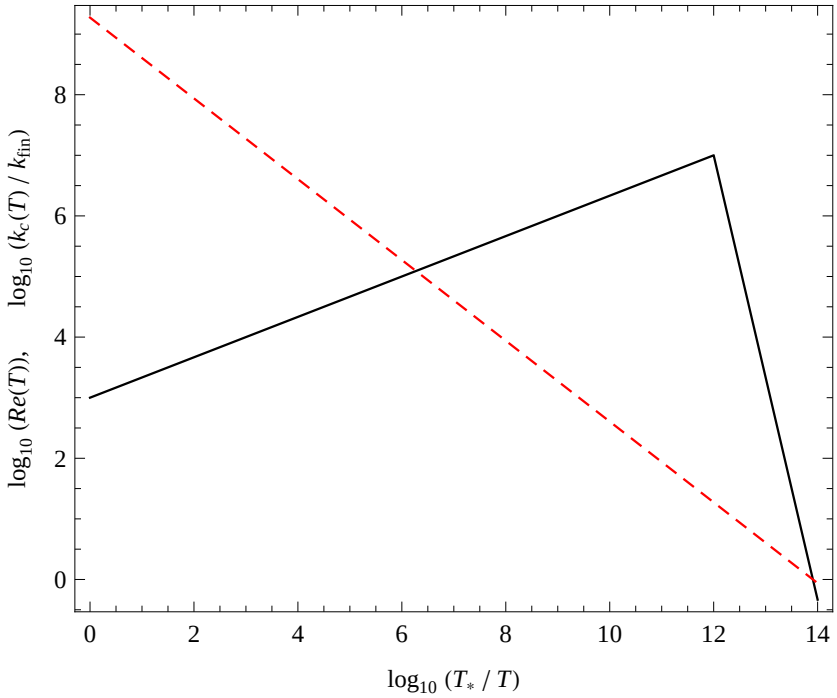

Figure 6. The Reynolds number $\mathrm{Re}(T)$ (black solid) and the comoving correlation scale $k_c(T)$ (red dashed) are shown in log scale as a function of $\log(T_*/T)$ with $T_* = 10^{14}\,\mathrm{GeV}$. Turbulence and with it the inverse cascade terminate at $T_{\rm fin} \simeq 1\,\mathrm{GeV}$ and $k_{\rm fin} = k_c(t_{\rm fin}) \simeq (10^{-12}\,\mathrm{Mpc})^{-1}$.

while the total energy density is reduced by the same factor such that $\widetilde{\rho}_B/k_c$ remains constant.

To compute the ratio $T_{\rm fin}/T_*$ we need to determine the temperature at which the Reynolds number becomes unity. In Appendix A of Ref. [23] the Reynolds number at very high temperatures is estimated to be

$$\mathrm{Re}(k,T) \;\propto\; \frac{aT}{k}\sqrt{\frac{\widetilde{\rho}_B(k)}{\rho_f}}$$

for a given scale k. Here ρ_f is the energy density of the fluid which contributes to the turbulent motion. In perfect thermal equilibrium $\rho_f = \rho$. More precisely, denoting the Reynolds number at the beginning of the inverse cascade by $R_* = \mathrm{Re}(k_c(t_*), T_*)$, it is found

$$\mathrm{Re}(k_c(T),T) \;=\; \begin{cases} R_* \left(\frac{T_*}{T}\right)^{1/3} & \text{for} \;\; T > T_{\rm ew} = 100\,\mathrm{GeV} \\ R_* \left(\frac{T_*}{T_{\rm ew}}\right)^{1/3} \left(\frac{T}{T_{\rm ew}}\right)^{11/3} & \text{for} \;\; T < T_{\rm ew}\,. \end{cases} \tag{66}$$

Setting $g_* \simeq 200$ and $T_* = 10^{14}\,\mathrm{GeV}$ yields $R_* \simeq a_* T_*/k_c(t_*) \simeq \sqrt{3/(a_{SB} g_*)}\, m_P/T_* \sim \mathcal{O}(10^3)$. (For simplicity we have set $\widetilde{\rho}_B/\rho_f \sim 1$ for this value.) Note that after inflation, until the electroweak transition at $T_{\rm ew}$, the Reynolds number of the fluid is actually increasing. This comes from the fact that it is inversely proportional to the comoving

mean free path which is constant at early times. After the electroweak phase transition, collisions are much more strongly suppressed and the comoving mean free path grows like a^4, hence the Reynolds number decreases rapidly. For more details see Ref. [23]. In Fig. 6 we show the evolution of both, the Reynolds number and the correlation scale of the helical magnetic field distribution through the inverse cascade.

Finally, we can now derive the generic scaling of $T_{\rm fin}$ with the initial temperature T_*. With the scaling $k_{\rm fin} = k_*(T_{\rm fin}/T_*)^{2/3}$ and the help of Eq. (66) for the evolution of the Reynolds number, we find that the Reynolds number becomes unity and the inverse cascade stops at $T_{\rm fin}$ given by

$$\frac{T_{\rm fin}}{T_*} \simeq 10^{-14}\left(\frac{10^{14}\,{\rm GeV}}{T_*}\right)^{9/11}, \qquad \text{for} \quad T_* > T_{\rm ew} \tag{67}$$

so that

$$k_{\rm fin} \simeq 10^{12}\,{\rm Mpc}^{-1}\left(\frac{T_*}{10^{14}\,{\rm GeV}}\right)^{5/11}. \tag{68}$$

For $T_* = 10^{14}\,{\rm GeV}$ we obtain $T_{\rm fin} \simeq 1\,{\rm GeV}$ and the correlation scale moves by about 9 orders of magnitude from k_* to $k_{\rm fin}$, see also Fig. 6.

Now we can trace the magnetic field spectrum through the inverse cascade. The spectral shape on large scales remains unchanged [22]. At late time, $t > t_{\rm fin}$ we therefore obtain

$$\frac{d\widetilde{\rho}_B}{d\ln k}(t,k) \simeq \begin{cases} \frac{d\widetilde{\rho}_B}{d\ln k}(t_*,k_*)\left(\frac{k}{k_*}\right)^4\left(\frac{T_*}{T_{\rm fin}}\right)^2 & \text{for} \quad k < k_{\rm fin} \\ 0 & \text{else.} \end{cases} \tag{69}$$

With $T_*/T_{\rm fin} \simeq 10^{14}$ this yields and amplification of 28 orders of magnitude of the initial amplitude on scales larger than $1/k_{\rm fin}$.

For a generic spectral index n, Eq. (69) is replaced by, see [23],

$$\frac{d\widetilde{\rho}_B}{d\ln k}(t,k) \simeq \begin{cases} \frac{d\widetilde{\rho}_B}{d\ln k_*}(t_*,k_*)\left(\frac{k}{k_*}\right)^{n+3}\left(\frac{T_*}{T_{\rm fin}}\right)^{2(n+2)/3} & \text{for} \quad k < k_{\rm fin}\,,\ t > t_{\rm fin} \\ 0 & \text{else.} \end{cases} \tag{70}$$

Clearly, the smaller n, the less significant is the amplification by the inverse cascade and for $n = -2$ there is no amplification at all. For $n < -2$ the above result does not apply, see [23].

In our case, where $n = 1$, Eq. (58) now yields

$$\frac{d\widetilde{\rho}_B}{d\ln k}(t_*,k_*) \simeq 4\times 10^{-68}\,{\rm GeV}^4\,\mathcal{S}^2(f_N)\left(\frac{g_*}{200}\right)^{2/3}\left(\frac{T_*}{10^{14}\,{\rm GeV}}\right)^4$$

with which we arrive at

$$\frac{d\widetilde{\rho}_B}{d\ln k}(t_{\rm fin},k_{\rm fin}) \simeq 2\times 10^{-77}\,{\rm GeV}^4\left(\frac{T_*}{10^{14}\,{\rm GeV}}\right)^{38/11}$$

where we assumed $g_* \simeq 200$. This determines the final strength of the magnetic field on large scales¶,

$$\widetilde{B}(k) \;\simeq\; 3\times10^{-19}\,\mathrm{Gauss}\,\mathcal{S}(f_N)\left(\frac{k}{k_{\mathrm{fin}}}\right)^2\left(\frac{T_*}{10^{14}\,\mathrm{GeV}}\right)^{19/11} \tag{71}$$

for $k \le k_{\mathrm{fin}}$. With the help of Eq. (68) this can also be written as

$$\widetilde{B}(k) \;\simeq\; 3\times10^{-19}\,\mathrm{Gauss}\,\mathcal{S}(f_N)\left(\frac{k}{10^{12}/\mathrm{Mpc}}\right)^2\left(\frac{T_*}{10^{14}\,\mathrm{GeV}}\right)^{9/11} \tag{72}$$

for $k \le k_{\mathrm{fin}}$.

After the end of the turbulent phase, magnetic fields are damped on small scales by viscosity and evolve by flux conservation, so that $\widetilde{B}$ = const. on large scales. For our typical value of $T_* \simeq 10^{14}\,\mathrm{GeV}$ hence $k_{\mathrm{fin}} \simeq 10^{12}/\mathrm{Mpc}$, for cosmologically interesting scales of $k \sim 10/\mathrm{Mpc}$ the magnetic field is of the order of $\widetilde{B}(k = 10/\mathrm{Mpc}) \simeq 10^{-40}\,\mathrm{Gauss}$. This is much too small for dynamo amplification. For smaller reheating temperatures, T_*, the Reynolds number grows less strongly and turbulence and the associated inverse cascade are of shorter duration. Therefore the value of $\widetilde{B}(k)$ at fixed $k < k_{\mathrm{fin}}$ is actually smaller for smaller T_*; the fact that k_* is larger in this case does not compensate this, see Eq. (72). Considering the lowest value for which our treatment is valid, $T_* \simeq T_{\mathrm{ew}} \simeq 100\,\mathrm{GeV}$ we arrive at $T_{\mathrm{fin}} \simeq 8\,\mathrm{MeV}$ and $k_{\mathrm{fin}} \simeq 4\times10^6/\mathrm{Mpc}$ but the magnetic field is only

$$\widetilde{B}(k) \;\simeq\; 6\times10^{-40}\,\mathrm{Gauss}\,\mathcal{S}(f_N)\left(\frac{k}{k_{\mathrm{fin}}}\right)^2, \quad \text{for} \quad k \le k_{\mathrm{fin}} \simeq 10^6/\mathrm{Mpc}\,. \tag{73}$$

At scales of 0.1 Mpc, this field is by far insufficient for subsequent dynamo amplification which requires seed fields of the order of at least $10^{-20}\,\mathrm{Gauss}$ [20]. For an arbitrary reheating temperature T_* we obtain from (72)

$$\widetilde{B}(k = 10/\mathrm{Mpc}) \;\simeq\; 3\times10^{-41}\,\mathrm{Gauss}\,\mathcal{S}(f_N)\left(\frac{T_*}{10^{14}\,\mathrm{GeV}}\right)^{9/11} \tag{74}$$

To achieve the minimal necessary field for dynamo amplification we would need $\mathcal{S}(f_N) \simeq 10^{21}$, an amplitude at which back-reaction after inflation would be very relevant and our treatment would therefore not be adequate.

Until recombination fields on scales smaller than about 10 kpc are damped by viscosity. The scales $k \gtrsim 100/\mathrm{Mpc}$ therefore do not survive the linear regime and will not be amplified before damping. But even on these smallest "surviving scales" the magnetic field generated is far too weak for dynamo amplification.

7. Conclusions

In this work, we have studied the generation of helical magnetic fields during inflation by adding a parity-breaking term of the form $f(\phi)F\widetilde{F}$ to the action. For the two choices of

¶ The magnetic field strength is $B = \sqrt{8\pi\rho_B}$ in Gauss units, where $\mathrm{GeV}^2 \simeq 1.4\times10^{19}\,\mathrm{Gauss}$, while in Heaviside-Lorentz units we have $B = \sqrt{2\rho_B}$ and $\mathrm{GeV}^2/\sqrt{4\pi} \simeq 1.4\times10^{19}\,\mathrm{Gauss}$.

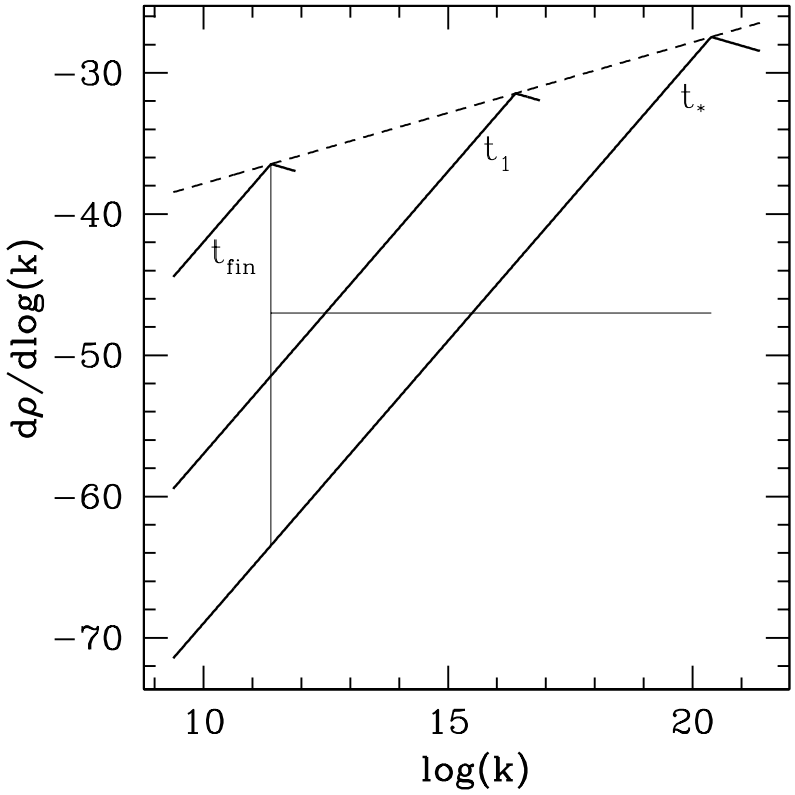

Figure 7. The process of inverse cascade is indicated. We show $\frac{d\widetilde{\rho}_B}{d\log(k)}(k_c(t),t)$ as a function of $k_c(t)$ (dashed line) as well as $\frac{d\widetilde{\rho}_B}{d\log(k)}(k,t_*)$, $\frac{d\widetilde{\rho}_B}{d\log(k)}(k,t_1)$ and $\frac{d\widetilde{\rho}_B}{d\log(k)}(k,t_{\rm fin})$ as functions of k (thick solid lines). We choose $t_1/t_* = 10^6$. The parts of the curves on the right side of the maximum are not reliable. The vertical line indicates the total amplification factor which is constant for $k < k_0 = k(t_{\rm fin})$. The horizontal line indicates the amount by which the correlation scale increases during the inverse cascade. The energy density is in units of Gauss^2 for $\mathcal{S}(f_N) = 1$ and k is in units of Mpc^{-1}.

the coupling function $f(\phi)$, namely a power law and an exponential form, we found that, during slow roll inflation, the power spectrum of the generated magnetic fields is always blue with spectral index $n = 1$. We have also studied the effects of a short deviation from slow roll. Such a departure from slow roll, if kept within the bounds allowed by the CMB data, does not strongly modify the overall shape of the magnetic field power spectrum. In principle, a very steep coupling function, e.g. a double-exponential $f(\phi) = f_0 \exp(\exp(\alpha\phi/m_P))$, can lead to a different spectrum, $n \neq 1$. However, for our requirement $|f(\phi)| \leq 1$, such a behaviour can be valid only over a short period of time. In the absence of a convincing physical motivation, we have therefore not investigated such an extreme case.

After inflation and reheating, an inverse cascade sets in and moves power from the correlations scale $k_* \simeq \mathcal{H}_*$ to larger scales, which is schematically represented in Fig. 7. We find that typical values for the reheating temperature, e.g. $T_* \simeq 10^{14}\,\mathrm{GeV}$ can only

lead to magnetic fields of the order 10^{-40} Gauss on scales of 0.1 Mpc and smaller values are obtained for smaller reheating temperatures. These field amplitudes are largely insufficient for dynamo amplification [20].

This result is quite generic. Power law or exponential couplings to an $F\widetilde{F}$ term during inflation cannot generate fields which may have provided the seeds for the large scale magnetic fields in galaxies and clusters. Even though for helical fields an inverse cascade does move power to larger scales, this is still largely insufficient. To obtain sufficient fields on large scales after the inverse cascade, they must have been so large on small scales after inflation that back-reaction cannot be neglected. Another possibility might be a very steep coupling which can lead to a different, $n \neq 1$ spectrum. However, only if the spectrum is close to scale invariant, it can have significant amplitudes on large scale without significant back-reaction from small scales.

The scenarios of inflationary magnetogenesis are often constrained by requiring that the back-reaction of the generated magnetic field on the background evolution is small. Since the perturbations in the scalar field are affected by the presence of a non-minimal coupling as indicated in Eq. (19), it will be interesting to study the back-reaction effects of the EM perturbations on the evolution of the primordial curvature perturbations. This may provide another tool to constrain inflationary scenarios of magnetogenesis. This issue will be addressed in a future project [35].

Acknowledgments

The authors acknowledge financial support from the Swiss National Science Foundation. R.K.J. acknowledges a research fellowship from the Indo Swiss Joint Research Program with grant no. RF 12.

Appendix A. Quantisation of the vector potential

Always working in Coulomb gauge, we promote the vector potential A_i to a quantum mechanical operator, define conjugate momentum as $\Pi^i \equiv \delta S/\delta \dot{A}_i$, and impose the commutation relation

$$\left[A_i(t,\boldsymbol{x}),\ \Pi^j(t,\boldsymbol{y})\right] \ = \ i\delta^j_{\perp i}(\boldsymbol{x}-\boldsymbol{y})\,. \tag{A.1}$$

Here the transversal Dirac delta, $\delta^j_{\perp i}$, is defined as

$$\delta^j_{\perp i}(\boldsymbol{x}-\boldsymbol{y}) \ \equiv \ \int \frac{d^3k}{(2\pi)^3} e^{i\boldsymbol{k}\cdot(\boldsymbol{x}-\boldsymbol{y})}\left(\delta^j_i - \hat{k}_i\hat{k}_m\delta^{mj}\right) \tag{A.2}$$

with $\hat{k}_i \equiv k_i/k$ and $k \equiv |\boldsymbol{k}|$. Let us compute the conjugate momentum in terms of the vector potential which we expand in terms of creation and annihilation operators in Fourier space. The canonical commutation relations of the creation and annihilation operators, together with the above commutation relation of A_i and Π^j will lead to a Wronskian normalisation condition on the mode functions of the quantised vector potential.

The conjugate momenta in the perturbed FL metric are

$$\Pi^i \;=\; a^2 g^{ij}\left(\dot{A}_j + f(\varphi)\epsilon_{jmn}\partial_m A_n\right) . \tag{A.3}$$

The non-standard second term arises due to the axial coupling of the EM field to the inflaton. Since it involves the curl of the vector potential it is convenient to expand the operators in Fourier space with respect to a helicity basis. For each comoving wave vector, $\boldsymbol{k}$, we define the comoving right-handed orthonormal basis

$$e^0_\mu \;\equiv a\Big(1,\,\mathbf{0}\Big)\,, \quad e^{1,2}_\mu(\boldsymbol{k}) \;\equiv\; a\Big(0,\,\boldsymbol{\varepsilon}^{\boldsymbol{k}}_{1,2}\Big)\,, \quad e^3_\mu(\boldsymbol{k}) \;\equiv a\Big(0,\,\hat{\boldsymbol{k}}\Big) \tag{A.4}$$

with

$$\hat{\boldsymbol{k}}\cdot\boldsymbol{\varepsilon}^{\boldsymbol{k}}_{1,2} \;=\; 0 \;=\; \boldsymbol{\varepsilon}^{\boldsymbol{k}}_1\cdot\boldsymbol{\varepsilon}^{\boldsymbol{k}}_2\,, \qquad \boldsymbol{\varepsilon}^{\boldsymbol{k}}_1\wedge\boldsymbol{\varepsilon}^{\boldsymbol{k}}_2 \;=\; \hat{\boldsymbol{k}}\,. \quad |\boldsymbol{\varepsilon}^{\boldsymbol{k}}_i|^2 = 1 \tag{A.5}$$

and

$$\boldsymbol{\varepsilon}^{-\boldsymbol{k}}_1 \;=\; -\boldsymbol{\varepsilon}^{\boldsymbol{k}}_1\,, \qquad \boldsymbol{\varepsilon}^{-\boldsymbol{k}}_2 \;=\; \boldsymbol{\varepsilon}^{\boldsymbol{k}}_2\,. \tag{A.6}$$

The two transverse directions are combined to the helicity (or circular) directions

$$\boldsymbol{\varepsilon}^{\boldsymbol{k}}_\pm \;\equiv\; \frac{1}{\sqrt{2}}\left(\boldsymbol{\varepsilon}^{\boldsymbol{k}}_1 \pm i\boldsymbol{\varepsilon}^{\boldsymbol{k}}_2\right) . \tag{A.7}$$

These have the following useful properties

$$\boldsymbol{\varepsilon}^{\boldsymbol{k}*}_\pm \;=\; \boldsymbol{\varepsilon}^{\boldsymbol{k}}_\mp \tag{A.8}$$

$$\boldsymbol{\varepsilon}^{-\boldsymbol{k}}_\pm \;=\; -\boldsymbol{\varepsilon}^{\boldsymbol{k}}_\mp \tag{A.9}$$

$$i\hat{\boldsymbol{k}}\wedge\boldsymbol{\varepsilon}^{\boldsymbol{k}}_\pm \;=\; \pm\boldsymbol{\varepsilon}^{\boldsymbol{k}}_\pm \tag{A.10}$$

$$\boldsymbol{\varepsilon}^{\boldsymbol{k}}_h\cdot\boldsymbol{\varepsilon}^{\boldsymbol{k}*}_{h'} \;=\; \delta_{hh'} \tag{A.11}$$

$$\sum_h \varepsilon^{\boldsymbol{k}}_{h,i}\,\varepsilon^{\boldsymbol{k}}_{h,j} \;=\; \delta_{ij} - \hat{k}_i\hat{k}_j \tag{A.12}$$

where $h, h' \in \{+,-\}$ and the star denotes complex conjugation. We now expand the vector potential in Fourier space in the helicity basis.

$$\begin{aligned} A_j(t,\boldsymbol{x}) \;=\; \int\frac{d^3k}{(2\pi)^3}\sum_{h=\pm}\Big\{ & e^h_j(\boldsymbol{k})b_h(\boldsymbol{k})A_h(t,k)e^{i\boldsymbol{k}\cdot\boldsymbol{x}} \\ & + e^{h*}_j(\boldsymbol{k})b^\dagger_h(\boldsymbol{k})A^*_h(t,k)e^{-i\boldsymbol{k}\cdot\boldsymbol{x}}\Big\} \end{aligned} \tag{A.13}$$

where the creation and annihilation operators, $b^\dagger_h(\boldsymbol{k})$ and $b_h(\boldsymbol{k})$, satisfy the canonical commutation relations

$$\Big[b_h(\boldsymbol{k}),\, b^\dagger_{h'}(\boldsymbol{q})\Big] \;=\; (2\pi)^3\delta^3(\boldsymbol{k}-\boldsymbol{q})\,\delta_{hh'} \tag{A.14}$$

$$\Big[b_h(\boldsymbol{k}),\, b^\dagger_{h'}(\boldsymbol{q})\Big] \;=\; 0 \;=\; \Big[b^\dagger_h(\boldsymbol{k}),\, b^\dagger_{h'}(\boldsymbol{q})\Big]\,. \tag{A.15}$$

The vacuum, $|0\rangle$, is defined by $b_h(\boldsymbol{k})|0\rangle \equiv 0$. As a consequence of the commutation relation (A.1) of A_i and its conjugate momentum, Π^j, as given in (A.3), the mode function must satisfy the Wronskian normalisation condition. In terms of the rescaled Fourier modes of the vector potential, $\mathcal{A}_h(t,k) \equiv aA_h(t,k)$, this reads

$$\dot{\mathcal{A}}_h(t,k)\mathcal{A}^*_h(t,k) - \mathcal{A}^*_h(t,k)\dot{\mathcal{A}}_h(t,k) \;=\; i\,. \tag{A.16}$$

Finally, the evolution equation for the Fourier modes can now be derived from the forced wave equation of the vector potential, Eq. (18),

$$\ddot{\mathcal{A}}_h(t,k) + \left[k^2 + hkf'(\varphi)\dot{\varphi}\right]\mathcal{A}_h(t,k) \;=\; 0 \tag{A.17}$$

where $h = \pm$ reflects the two helicity modes.

Appendix B. Asymptotic behaviour of the Coulomb wave functions

To investigate the late time behaviour of the solution to the mode equation for a power law coupling, we need asymptotic expressions for the Coulomb wave function, $G_0(y,x)$ and $F_0(y,x)$, for $x \to 0$. Based on their expansion in terms of Bessel functions given in Abramowitz & Stegun [37], we derive the asymptotes of G_0, F_0, G_0', F_0' for $x \to 0$ for arbitrary but fixed y. Actually, we argue that the asymptotic limits for $x \ll 2y$ given in 14.6.9-10 (p. 542) of [37] are incorrect. All statements given here were verified numerically using *Mathematica* [46] and *Maple* [47].

We start from the asymptotic expressions in terms of the modified Bessel functions, K and I, given in 14.6.7 of [37] for $L = 0$, and $2y \gg x$

$$G_0(y,x) \;\simeq\; 2\sqrt{2xy}\,W(y)K_1(2\sqrt{2xy}) \tag{B.1}$$

$$F_0(y,x) \;\simeq\; \frac{x}{\sqrt{2xy}}W(y)^{-1}\,I_1(2\sqrt{2xy}) \tag{B.2}$$

where (see C_0 given in 14.1.8 of [37])

$$W(y) \;\equiv\; \left[\frac{e^{\pi y}\sinh(\pi y)}{\pi y}\right]^{1/2}. \tag{B.3}$$

We notice that the approximations given in 14.6.8 of A&S, where

$$\sinh \pi y \;\simeq\; \frac{1}{2}e^{\pi y} \tag{B.4}$$

is used, are only accurate to better than 1% if $y \gtrsim 1$. Since in our case y is arbitrary or rather smaller than unity, we cannot employ this approximation. As for the x-derivatives of G_0 and F_0 we have verified numerically that the derivatives of the above expressions are good approximations,

$$G_0'(y,x) \;\simeq\; -4yW(y)\,K_0(2\sqrt{2xy}) \tag{B.5}$$

$$F_0'(y,x) \;\simeq\; W(y)^{-1}\,I_0(2\sqrt{2xy})\,. \tag{B.6}$$

Next we use the asymptotic properties of the modified Bessel functions for *small* arguments. As given on p. 375 in [37]

$$K_1(z) \;\simeq\; 1/z + \mathcal{O}(z)\,, \qquad K_0(z) \;\simeq\; -\ln(z/2) - \gamma_E + \mathcal{O}(z^2) \tag{B.7}$$

$$I_1(z) \;\simeq\; z/2 + \mathcal{O}(z^3)\,, \qquad I_0(z) \;\simeq\; 1 + \mathcal{O}(z^2) \tag{B.8}$$

for $z = 2\sqrt{2xy} \ll 1$. Using these expressions we find to lowest order in x for $x \ll (8y)^{-1}$

$$G_0(y,x) \;\simeq\; W(y)\,, \qquad G_0'(y,x) \;\simeq\; 2yW(y)\ln(2xy) \tag{B.9}$$

$$F_0(y,x) \;\simeq\; x/W(y)\,, \qquad F_0'(y,x) \;\simeq\; 1/W(y)\,. \tag{B.10}$$

These asymptotic expressions differ significantly from those given in 14.6.9-10 of [37] and it is straightforward to understand why: one arrives at the expressions of [37] when falsely using the asymptotic expansions of the modified Bessel functions for *large* arguments, where $I_1(|z| \gg 1) \simeq e^z/\sqrt{2\pi z}$ and $K_1(|z| \gg 1) \simeq e^{-z}\sqrt{\pi/(2z)}$. However, for $x \to 0$ and fixed y, $z = 2\sqrt{2xy}$ tends to zero and is not large as assumed for approximations 14.6.9-10 of [37].

References

[1] P. P. Kronberg, Rept. Prog. Phys. **57**, 325 (1994).
[2] L. Pentericci, W. Van Reeven, C. L. Carilli, H. J. A. Rottgering and G. K. Miley, Astron. Astrophys. Suppl. Ser. **145**, 121 (2000), [astro-ph/0005524].
[3] N. Battaglia, C. Pfrommer, J. L. Sievers, J. R. Bond and T. A. Ensslin, Mon. Not. Roy. Astron. Soc. **393**, 1073 (2009), [0806.3272].
[4] T. E. Clarke, P. P. Kronberg and H. Boehringer, Astrophys. J. **547**, L111 (2001), [astro-ph/0011281].
[5] J. Lee, U.-L. Pen, A. R. Taylor, J. M. Stil and C. Sunstrum, 0906.1631.
[6] A. Neronov and I. Vovk, Science **328**, 73 (2010).
[7] K. Takahashi, K. Ichiki, H. Ohno, H. Hanayama and N. Sugiyama, astro-ph/0601243.
[8] K. Ichiki, K. Takahashi, N. Sugiyama, H. Hanayama and H. Ohno, Mod. Phys. Lett. **A22**, 2091 (2007).
[9] S. Maeda, S. Kitagawa, T. Kobayashi and T. Shiromizu, Class. Quant. Grav. **26**, 135014 (2009), [0805.0169].
[10] K. Enqvist and P. Olesen, Phys. Lett. **B319**, 178 (1993), [hep-ph/9308270].
[11] M. Joyce and M. E. Shaposhnikov, Phys. Rev. Lett. **79**, 1193 (1997), [astro-ph/9703005].
[12] M. M. Forbes and A. R. Zhitnitsky, Phys. Rev. Lett. **85**, 5268 (2000), [hep-ph/0004051].
[13] T. Boeckel and J. Schaffner-Bielich, 0906.4520.
[14] R. Durrer and C. Caprini, JCAP **0311**, 010 (2003), [astro-ph/0305059].
[15] C. Caprini and R. Durrer, Phys. Rev. **D65**, 023517 (2001), [astro-ph/0106244].
[16] K. Subramanian, Astron. Nachr. **331**, 110 (2010), [0911.4771].
[17] J. Martin and J. Yokoyama, JCAP **0801**, 025 (2008), [0711.4307].
[18] V. Demozzi, V. Mukhanov and H. Rubinstein, JCAP **0908**, 025 (2009), [0907.1030].
[19] R. Durrer, New Astron. Rev. **51**, 275 (2007), [astro-ph/0609216].
[20] A. Brandenburg and K. Subramanian, Phys. Rept. **417**, 1 (2005), [astro-ph/0405052].
[21] R. Banerjee and K. Jedamzik, Phys. Rev. **D70**, 123003 (2004), [astro-ph/0410032].
[22] L. Campanelli, Phys. Rev. Lett. **98**, 251302 (2007), [0705.2308].
[23] C. Caprini, R. Durrer and E. Fenu, JCAP **0911**, 001 (2009), [0906.4976].
[24] T. Vachaspati, Phys. Rev. Lett. **87**, 251302 (2001), [astro-ph/0101261].
[25] C. Caprini, R. Durrer and T. Kahniashvili, Phys. Rev. **D69**, 063006 (2004), [astro-ph/0304556].
[26] N. Seto and A. Taruya, Phys. Rev. **D77**, 103001 (2008), [0801.4185].
[27] J. M. Cornwall, Phys. Rev. **D56**, 6146 (1997), [hep-th/9704022].
[28] G. B. Field and S. M. Carroll, Phys. Rev. **D62**, 103008 (2000), [astro-ph/9811206].
[29] L. Campanelli and M. Giannotti, Phys. Rev. Lett. **96**, 161302 (2006), [astro-ph/0512458].
[30] L. Campanelli and M. Giannotti, Phys. Rev. **D72**, 123001 (2005), [astro-ph/0508653].
[31] M. M. Anber and L. Sorbo, JCAP **0610**, 018 (2006), [astro-ph/0606534].
[32] L. Campanelli, Int. J. Mod. Phys. **D18**, 1395 (2009), [0805.0575].
[33] M. Giannotti and E. Mottola, Phys. Rev. **D79**, 045014 (2009), [0812.0351].
[34] R. Durrer, *The Cosmic Microwave Background* (Cambridge University Press, Cambridge, UK, 2008).
[35] R. Durrer, L. Hollenstein and R. K. Jain, In preparation (2010).

[36] J. D. Barrow, R. Maartens and C. G. Tsagas, Phys. Rept. **449**, 131 (2007), [astro-ph/0611537].

[37] M. Abramowitz and I. A. Stegun, *Handbook of Mathematical Functions* (Dover, New York, USA, 1972).

[38] L. Covi, J. Hamann, A. Melchiorri, A. Slosar and I. Sorbera, Phys. Rev. **D74**, 083509 (2006), [astro-ph/0606452].

[39] J. Hamann, L. Covi, A. Melchiorri and A. Slosar, Phys. Rev. **D76**, 023503 (2007), [astro-ph/0701380].

[40] M. J. Mortonson, C. Dvorkin, H. V. Peiris and W. Hu, Phys. Rev. **D79**, 103519 (2009), [0903.4920].

[41] R. K. Jain, P. Chingangbam, J.-O. Gong, L. Sriramkumar and T. Souradeep, JCAP **0901**, 009 (2009), [0809.3915].

[42] R. K. Jain, P. Chingangbam, L. Sriramkumar and T. Souradeep, 0904.2518.

[43] D. K. Hazra, M. Aich, R. K. Jain, L. Sriramkumar and T. Souradeep, 1005.2175.

[44] J. A. Adams, B. Cresswell and R. Easther, Phys. Rev. **D64**, 123514 (2001), [astro-ph/0102236].

[45] D. Biskamp, *Magnetohydrodynamic Turbulence* (Cambridge University Press, Cambridge, UK, 2003).

[46] Wolfram Research, Inc., *Mathematica: Version 7.0* (Wolfram Research, Inc., Champaign, Illinois, USA, 2008).

[47] Maplesoft, *Maple: Version 13.02* (Maplesoft, a division of Waterloo Maple Inc., Waterloo, Ontario, Canada, 2009).